Inherent Limitations of Volumetric Solar Receivers

A. Kribus
Weizmann Institute of Science, Environmental Sciences and Energy Research Department, Rehovot 76100, Israel

H. Ries
Paul Scherrer Institute, CH-5232 Villigen, Switzerland

W. Spirkl
Ludwig-Maximilians-Universität, Sektion Physik, Amalienstr. 54, D-80799 München, Germany

The flow in volumetric absorbers is investigated using a simple mathematical model. It is found that there are several restrictions and failure mechanisms that are inherent to the volumetric absorber, regardless of the precise structural details, material properties, etc. The heat that the absorber can extract safely is limited by flow-related constraints. Multiple steady solutions exist for certain parameter values: a "fast" solution corresponding to a low exit temperature, a "slow" solution which is unstable, and a "choked" solution for which the absorber is near to stagnation temperature. The existence of multiple solutions may lead to abrupt local "switching" and absorber failure. For a given irradiance applied to the absorber, the existence and the character of the solutions are determined by a single dimensionless parameter, the Blow parameter B. *Neglecting the variation of the hydraulic resistivity with temperature may lead to a dangerous overestimate of the receiver's ability to sustain irradiation. For reasonable efficiencies control of mass flow or outlet temperature of the absorber, rather than pressure control, may be required.*

1 Introduction

Solar receivers with volumetric absorbers have become very popular in recent years. These absorbers offer several advantages such as spreading the radiation absorption process over the depth of the absorber, thus increasing heat transfer area and reducing the local flux density on absorbing surfaces; reducing re-radiation losses by lowering the outward-facing surfaces' temperature; simple and flexible construction; and some offer structures with low thermal stresses. Several kinds of volumetric absorbers have been built and tested, for example, porous ceramic (Buck et al., 1991), metallic wire mesh (Fricker et al., 1988; Heinrich et al., 1992), ceramic fibers (Buck, 1988), ceramic grid (Posnansky et al., 1991; Bohmer et al., 1991; Pitz-Paal et al., 1992), packed bed of particles (Menigault et al., 1991), and "Porcupine" (Karni et al., 1992).

Many of the experiments with volumetric absorbers, and especially those with open (atmospheric) receivers, have suffered considerably from nonuniform flow conditions and persistent local overheating. In some cases these local effects have led to failure (e.g., melting, cracking) of the absorber. The prevailing opinion is that these local failures are due to nonuniformities of either the receiver or the radiation, and may be overcome by compensating the hydraulic resistance at different locations across the absorber.

We show in this work that the volumetric absorber has inherent limitations, and is prone to failure under certain conditions. The flow through a volumetric absorber exhibits multiple steady-state solutions, with the possibility of sudden hysteresis-type switching, an inherent limit on allowable irradiation, and the possibility of flow instability.

In the analysis of these limitations, an important property which is often overlooked is the variation of the fluid's dynamic viscosity with temperature. We find that this variation plays a significant role in determining the maximum allowable irradiance on a volumetric absorber. Using the viscosity at inlet temperature leads to a dangerous overestimation (by a factor of 3) of the maximum allowable irradiance. Furthermore, the variation of the viscosity with temperature may yield multiple steady-state solutions.

In the next section, the model describing flow and energy transfer through a volumetric absorber is constructed. The following two sections present steady, one-dimensional solutions for two cases: constant heat source and variable, temperature-dependent heat source.

2 A Model of a Volumetric Absorber

Consider the volumetric absorber as a solid matrix, through which gas flows continuously. The solid phase serves as a heat source for the gas phase as shown in Fig. 1. In most volumetric absorbers the solid fraction is small enough for these approximations to hold. The conservation of mass (continuity) for the gas is

$$\frac{\partial \rho}{\partial t} + \nabla \cdot (\rho \mathbf{u}) = 0, \tag{1}$$

where ρ is the density and $\mathbf{u}$ the average velocity of the gas. The momentum balance is dominated by viscous (molecular diffusion) processes when the local Reynolds number is not much larger than 1, as in fact occurs in wire-mesh and ceramic fiber absorbers. The velocity is then proportional to the pressure gradient, as in the well-known relations for Stokes flow or Darcy flow (Batchelor, 1967): $r\mathbf{u} = -\nabla p$. The "hydraulic resistivity" r is proportional to the fluid's dynamic viscosity, and p is the pressure. In ceramic grid or Porcupine absorbers the Reynolds number may be of order 10 or 100, and the momentum equation must be modified. Strictly the present analysis applies only to low Reynolds numbers. However, for a modified momentum equation, e.g., with an additional term proportional to the density and to the square of the velocity, the following analysis may be carried out in an analogous manner, and qualitatively similar phenomena are observed.

In a solar receiver, the fluid's temperature T may change over a wide range, causing significant changes in viscosity from inlet to outlet. For practical purposes, this dependence may be described by a power law: $r \propto T^{\omega}$ (Schlichting, 1979). For air at high temperatures, the value $\omega = 0.7$ is appropriate. For an ideal gas, with an interaction cross section σ which does not depend on temperature, $\omega = 0.5$, and assuming $\sigma \propto 1/\sqrt{T}$ for lower temperatures yields $\omega = 1$ (Landau et al., 1983).

The momentum balance becomes

$$r(T)\mathbf{u} = r_i \frac{T^{\omega}}{T_i^{\omega}} \mathbf{u} = -\nabla p. \tag{2}$$

For the equation of state we use the ideal gas approximation:

Contributed by the Solar Energy Division of THE AMERICAN SOCIETY OF MECHANICAL ENGINEERS for publication in the ASME JOURNAL OF SOLAR ENERGY ENGINEERING. Manuscript received by the ASME Solar Energy Division, Sept. 94; final revision, May 1995. Associate Technical Editor: J. H. Davidson.

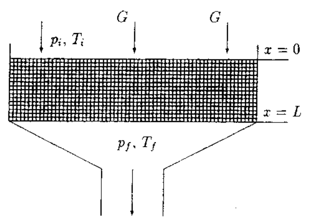

Fig. 1 Schematic of a volumetric absorber. Fluid enters the absorber at $x = 0$ with inlet pressure p_i and inlet temperature T_i. The absorber transfers the heat flux density G to the fluid, the fluid exits with outlet pressure p_f and outlet temperature T_f at $x = L$.

$$p = \rho RT. \tag{3}$$

An energy balance over a control volume in the absorber, neglecting conduction in both the gas and the solid, yields an equation for the enthalpy per unit volume of the gas:

$$\frac{\partial h}{\partial t} + \nabla \cdot (\mathbf{u}h) = \left(S - c_A \frac{\partial T}{\partial t}\right). \tag{4}$$

The left-hand side is the substantial derivative for the fluid's enthalpy. The right-hand side combines the net absorbed radiation S and the energy stored in the solid matrix to an effective net source for the fluid. Here c_A is the specific heat of the absorber matrix per unit volume. With the right-side zero this corresponds to the Joule-Thompson effect, which yields zero temperature change for an ideal gas (this can be verified by eliminating p with T). Ideally a volumetric receiver has a much larger area for heat transfer to the fluid than for absorption of radiation. With this idealization in mind we assume that the temperatures of the absorber and the fluid are equal.

In the analysis below we substituted the enthalpy h with the pressure p using Eq. (3):

$$h = \frac{\gamma}{\gamma - 1} p, \tag{5}$$

where γ is the ratio of gas heat capacity for constant pressure to that for constant volume.

The boundary conditions are known state of the fluid at the inlet, p_i and T_i, and imposed pressure p_f at the outlet. Without loss of generality, we set $p_i \geq p_f$; the case of $p_i < p_f$, with T_f specified, is identical except that the flow proceeds in the opposite direction.

3 Steady, One-Dimensional Solutions

The fundamental case for steady state is a one-dimensional flow, as in a flat absorber facing the radiation field with a uniform pressure difference across the absorber (Heinrich et al., 1992). Even a curved absorber is usually thin enough relative to its radius of curvature for the flow to be considered locally one-dimensional. Equations (1), (2), and (4) then become

$$\frac{d(\rho u)}{dx} = 0 \tag{6}$$

$$ru = -\frac{dp}{dx} \tag{7}$$

$$\frac{d(pu)}{dx} = \frac{\gamma - 1}{\gamma} S. \tag{8}$$

The mass flux density $j = \rho u$ is obtained from Eqs. (3) and (7):

$$j = -p \frac{dp}{dx} \frac{1}{rTR}. \tag{9}$$

Substitute Eqs. (3) and (6) into Eq. (8) to obtain

$$jR \frac{dT}{dx} = \frac{\gamma - 1}{\gamma} S. \tag{10}$$

3.1 Constant Heat Source Density. For the sake of simplicity, we consider a constant heat source density S. Then Eq. (10) has a solution in which the temperature increases linearly with the depth:

$$T(x) = T_i\left(1 + a\frac{x}{L}\right). \tag{11}$$

Here a is the relative increase in temperature from inlet to outlet,

$$a \equiv \frac{T_f - T_i}{T_i} = \frac{\gamma - 1}{\gamma} \frac{G}{jRT_i}, \tag{12}$$

and $G = SL$ is the absorbed solar irradiance. The relative temperature increase a (and thus j) is determined by integrating Eq. (9) to obtain the solution for the pressure

$$p^2(0) - p^2(x) = 2jR \int_0^x rTdx'. \tag{13}$$

Equation (11) and the boundary conditions for the pressure yield an equation for a (with $T(x') = T_i(1 + ax'/L)$):

$$\frac{\gamma}{\gamma - 1} \cdot \frac{p_i^2 - p_f^2}{GLr_i} = \frac{2}{aL} \int_0^L \frac{T}{T_i} \frac{r(T)}{r_i} dx'. \tag{14}$$

The expression on the left is proportional to the pressure difference across the absorber, and may be viewed as indicating the "strength" of the blowing action of the fan. We call this dimensionless expression the *Blow parameter B*:

$$B = \frac{\gamma}{\gamma - 1} \cdot \frac{p_i^2 - p_f^2}{GLr_i}. \tag{15}$$

Assuming $r \propto T^\omega$ the right-hand side of Eq. (14) can be expressed in closed form:

Nomenclature

a = relative temperature rise, $a = (T_f - T_i)/T_i$
B = Blow parameter
c_A = absorber specific heat per volume ($\mathrm{JK^{-1}m^{-3}}$)
G = net absorbed solar irradiance (power per area) ($\mathrm{Wm^{-2}}$)
h = enthalpy per unit volume ($\mathrm{Jm^{-3}}$)
j = mass flux density (per area and time) ($\mathrm{kgm^{-2}s^{-1}}$)
L = depth of the absorber (m)
p = pressure (Pa)
r = hydraulic resistivity ($\mathrm{Pa\,sm^{-2}}$)
R = specific gas constant, 287 $\mathrm{J\,kg^{-1}\,K^{-1}}$
S = heat source per unit volume ($\mathrm{Wm^{-3}}$)
T = absolute temperature (K)
$\mathbf{u}$ = velocity ($\mathrm{ms^{-1}}$)
γ = ratio of specific heats (C_p/C_v)
ρ = mass density ($\mathrm{kgm^{-3}}$)
ω = temperature exponent of resistivity $r \propto T^\omega$

Subscripts

i, f = inlet ($x = 0$), outlet ($x = L$)
ss = steady state
∞ = stagnation

$$B = f(a) \equiv \frac{2}{\omega + 2} \frac{(1 + a)^{\omega+2} - 1}{a^2} . \qquad (16)$$

The solution of Eq. (16) for a depends on the value of ω and on B. In Fig. 2 we plot the relation between the temperature increase a and the Blow parameter B. For given material, geometry, and radiation the Blow parameter is physically increased by increasing the action of the fan. For pressurized receivers this means increasing p_i. For open receivers this means lowering p_f. But for open receivers there is a physical limit: p_f cannot decrease below zero. For given initial and final pressure, B may be increased by decreasing the irradiance, i.e., concentration, and vice versa.

One would expect that increasing the Blow parameter would decrease the temperature. Indeed this is true for high enough Blow parameter and low relative temperatures. But for positive values of ω there is a regime where Eq. (16) formally implies a counter intuitive behavior: lower temperature requires less blowing. We show in the next section that in this regime the solution is not stable. There is a minimum Blow parameter B_{min}, below which there is no solution for a. This minimum value corresponds to an upper limit for the heat flux density that can be handled by a given volumetric receiver:

$$G \leq \frac{\gamma}{\gamma - 1} \cdot \frac{p_i^2 - p_f^2}{r_i L B_{min}} . \qquad (17)$$

When the heat source G increases, the temperature as well as the viscosity increase. This reduces the mass flow rate for the given pressure drop ("choking"), and reduces the heat removal capacity, providing a positive feedback for further temperature increase. Above some heat source threshold, the flow cannot remove the heat, and the solution ceases to exist, as seen in Fig. 2. Obviously, the constant heat source assumption is not valid at very high temperatures; this is treated in the next section.

The limit Eq. (17) is completely unrelated to the *material* limitations of the absorber structure; rather, it is a property of the *flow*. Figure 3 shows the dependence of B_{min} on ω. If the heat source applied to a given receiver is increased, then the steady-state solutions cease to exist when G exceeds the value in Eq. (17). In atmospheric receivers, the receiver inlet conditions (p_i, T_i) are fixed to ambient pressure and close to ambient temperature, respectively; the limitation (17) may then be severe, since p_f cannot be reduced below zero (in practical systems, p_f will be only slightly below p_i). On the other hand, if p_f is fixed while p_i is free to increase, as in pressurized receivers such as the DIAPR (Karni et al., 92) or VOBREC (Heller et al., 1992), then the limitation (17) may be relieved by increasing p_i as required.

Another advantage of working at high pressure concerns the power required for pumping. The Blow parameter depends on the difference in the *squares* of the pressures; thus for constant B the pressure drop is inversely proportional to the average pressure p. The volume flow is proportional to the pressure drop, thus the pumping power is proportional to $1/p^2$.

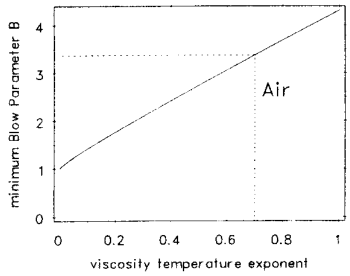

Fig. 3 Minimum Blow parameter B required for existence of steady flow solutions as a function of ω

Figure 2 also shows that, if $\omega > 0$, for any $B > B_{min}$ there are two solutions for a. According to Eq. (12), the solution with higher value of a will have higher temperatures and less mass flux density throughout the receiver. We therefore call the larger and smaller a solutions the "slow" and "fast" flows, respectively. The pressure and temperature profiles corresponding to the slow and fast flows for air ($\omega = 0.7$) and $B = 4$ are shown in Fig. 4.

For air ($\omega = 0.7$) solutions exist only if the Blow parameter exceeds 3.37. If the effect of temperature on the viscosity is neglected ($\omega = 0$), then the solution for a, and therefore for the pressure and temperature profiles, becomes unique. The limitation on B still exists, but is less severe than the case of $\omega = 0.7$ by a factor of about 3: $B \gtrsim 1$. The limit on the heat source G, derived by using the viscosity at inlet temperature, would not then be strict enough.

3.2 Temperature-Dependent Losses. In the previous section we assumed that the absorbed radiation is equivalent to a net heat source density independent of the temperature of the absorber. Neglecting re-radiation losses leads to an absorber temperature which increases indefinitely as the mass flow rate goes to zero. We now introduce radiative losses according to the Stefan law, so that the net source density at a certain temperature T is given by

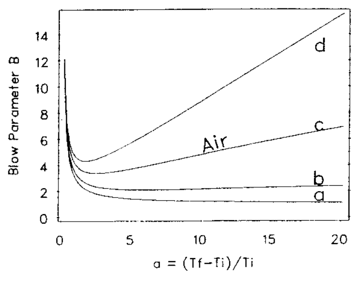

Fig. 2 Blow parameter B as function of the relative temperature increase a according to Eq. (16), for ω = 0 (a), 0.3 (b), 0.7 (c), and 1 (d). For given B, the smaller value of a represents the "fast" solution, the larger value the "slow" solution.

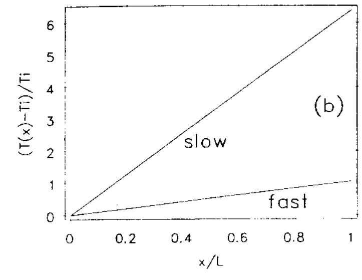

Fig. 4 (a) Pressure and (b) temperature profiles for ω = 0.7, B = 4, a = 6.39 ("slow" solution) and a = 1.047 ("fast" solution). The pressure is plotted as $\pi(x) = (p^2(x) - p_f^2)/(p_i^2 - p_f^2)$.

$$S(T) = S(0)\left[1 - \left(\frac{T}{T_\infty}\right)^4\right], \tag{18}$$

where T_∞ is the stagnation temperature at which the radiative losses equal the absorbed irradiance. From Eq. (10) it is seen that the temperature profile $T(x)$ is generally not linear. Strictly this model is only valid for optically thin absorbers, where the emission from a section of the absorber exits the receiver without interaction with the neighboring sections. The other limit, that of an optically thick absorber, is discussed below.

We eliminate j with Eq. (10):

$$j = \frac{L}{R\dfrac{\gamma}{\gamma - 1}} \frac{1}{\displaystyle\int_{T_i}^{T_f} \frac{dT}{S(T)}}. \tag{19}$$

Eliminate dx in Eq. (13) with Eq. (10):

$$p^2(0) - p^2(x) = 2j^2R^2\left(\frac{\gamma}{\gamma - 1}\right) \int_{T_i}^{T(x)} r(T')T' \frac{dT'}{S(T')}. \tag{20}$$

Set $x = L$, eliminate j with Eq. (19), and use again the relative temperature increase $a = (T_f - T_i)/T_i$:

$$p^2(0) - p^2(L) = 2\left(\frac{\gamma - 1}{\gamma}\right) \frac{L^2}{\left(\displaystyle\int_{T_i}^{T_f} \frac{dT}{S(T)}\right)^2} \times \int_{T_i}^{T_f} r(T)T\frac{dT}{S(T)} = \left(\frac{\gamma - 1}{\gamma}\right) Lr_iG_if(a), \tag{21}$$

where

$$f(a) = 2\frac{\displaystyle\int_{T_i}^{T_i(1+a)} \frac{r(T)}{r_i} \frac{T}{T_i} \frac{S_i}{S(T)} \frac{dT}{T_i}}{\left(\displaystyle\int_{T_i}^{T_i(1+a)} \frac{S_i}{S(T)} \frac{dT}{T_i}\right)^2}. \tag{22}$$

Here $G_i = LS_i$ is the net flux that would have been absorbed if the receiver were isothermal with temperature T_i. A generalized condition on B is now

$$B = f(a), \tag{23}$$

with $f(a)$ defined as in Eq. (22) and G_i used instead of G. For small a the function $f(a)$ is proportional to $1/a$, as for the case $dS/dT = 0$. In contrast to the former case, a is now restricted to $a < a_\infty = (T_\infty - T_i)/T_i$, and, owing to the divergence of the integrals with $dT/S(T)$, $f(a)$ approaches zero for $a \to a_\infty$. Thus there is either one solution or there are three solutions (two solutions occasionally coincide for $f'(a) = 0$ thus giving two solutions). This is depicted in Fig. 5 for the case $a_\infty = 10$; Fig. 2 thus corresponds to $a_\infty = \infty$. The leftmost solution branch in Fig. 5 (small a) corresponds to the "fast" solution. The intermediate region between the two turning points, when it exists (e.g., curves c and d), corresponds to the "slow" solution. The rightmost branch (a approaching a_∞) is called the "choked" solution, since its flow rate is close to zero.

For any B there is at least one solution, in contrast to the more limited case of constant heat source (Fig. 2). However, for small B only the "choked" solution is obtained. This solution corresponds to receiver exit temperature close to stagnation (which may exceed absorber material limitations), and flow rate close to zero (with net heat extracted and receiver efficiency also close to zero). The "choked" solution is therefore undesirable, and the value of B should be kept above the limit point

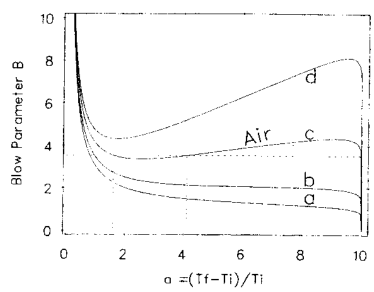

Fig. 5 Blow parameter B versus relative temperature rise a for radiative black-body losses $a_\infty = 10$, corresponding to, e.g., $T_i = 300$ K and $T_i = 3300$ K, for $\omega = 0$ (a), 0.3 (b), 0.7 (c), and 1 (d). Corresponding to the example given below, the values of a for $B = 3.527$ are indicated by dotted lines. For given B, the smaller value of a ($a = 1.6$, $T_f = 780$ K) represents the "fast" solution, the larger value ($a = 4.1$, $T_f = 1531$ K) the "slow" solution, and the value near to a_∞ ($a = 9.978$, $T_f = 3293$ K) the "choked" solution.

connecting the "fast" and "slow" branches (which we therefore still call B_{min}). In cases where the "slow" branch does not exist (e.g., curves a and b in Fig. 5), B_{min} is not well defined. It can be shown, however, that the receiver efficiency decreases monotonously with a; it is possible then to define B_{min} by the requirement that the receiver efficiency be higher than some specified value. This definition holds for all solutions, regardless of the value of ω. The positive feedback mechanism mentioned above is still visible in these results. The effect of including temperature-dependent losses is that the flow "choking" process does not proceed to infinite temperature, but equilibrates at a very low-flow (high-temperature) level, represented by the choked solution branch.

The structure of curves c and d in Fig. 5 suggests a hysteresis phenomenon. When the heat source gradually increases (B decreases), the solution will switch from the "fast" branch to the "choked" branch at the limit point B_{min}. It can be shown that the "slow" branch is unstable. When the heat source decreases, the "choked" solution will remain at higher values of B before switching back. This kind of transition may occur during daily variations of insolation or during cloud transitions.

For small ω, there is a unique solution for every $B > 0$. When $a_\infty = \infty$, this occurs only at $\omega = 0$. The smaller a_∞ the larger the maximum value ω for which this holds. Thus for low-concentration (low a_∞) volumetric receivers, such as those that have been constructed so far, the solution switching phenomenon is not dominant. However, higher-concentration receivers may enter the range of multiple solutions.

All solutions have a region where the slope $f'(a)$ is small, and small changes in the pressure will cause large changes in the exit temperature and receiver efficiency. A pressure controlled loop, whether atmospheric or pressurized, will need a very fine adjustment of the pressure difference. The solution for this control problem is to either increase operating pressure, thus increasing B for a given pressure drop and moving to the large-slope region, or to control flow rate or temperature rather than pressure.

3.3 Isothermal Absorber. When the absorber is not optically thin, there is radiative energy transfer between different locations of the absorber, which is equivalent to a heat conduction process in the flow direction. The absorber itself may also exhibit solid-phase heat conduction. However, heat conduction in the direction of flow does not at all decrease the minimum Blow parameter required. Assume, as an extreme case, an isothermal absorber. The fluid's temperature is then discontinuous, $T = T_i$ at $x < 0$, $T = T_f$ at $x > 0$. Equations (6) and (2) yield

$$j = \rho u = -\frac{p\dfrac{dp}{dx}}{RT_fr(T_f)} = \frac{p_i^2 - p_f^2}{2LRT_fr(T_f)}, \tag{24}$$

and Eq. (8) yields

$$\frac{\gamma - 1}{\gamma} LS(T_f) = jR(T_f - T_i). \quad (25)$$

This yields the implicit equation for a:

$$B = 2\left[\frac{r(T_i(1 + a))}{r(T_i)} \frac{S(T_i(1 + a))}{S(T_i)}\right] \frac{1 + a}{a} \equiv f(a). \quad (26)$$

Here B is defined as in Eq. (22), and $f(a)$ has properties similar to $f(a)$ in Eq. (22), but with other values for B. E.g., for $dS/dT = 0$ and $\omega = 0$, $B_{\min} = 2$, in contrast to the case of no heat conduction in flow direction, where $B_{\min} = 1$. Hence in an isothermal receiver a high pressure gradient is required throughout the receiver, even at the inlet, increasing the minimum B value for steady-state solutions. Even for $\omega > 0$ the ratio of the minimum Blow parameter $B_{\min}$ for the two cases is close to two.

4 A Practical Example

Future high temperature applications do require high concentration ratios and compact receivers at high power levels. The DIAPR (Karni et al., 1992) has been demonstrated at 10,000 suns. As an example we consider a high-concentration volumetric absorber with the data as in Table 1. We assume that, despite the high mass flux, due to small absorber structures the Reynolds number is low enough for Eq. (2) being valid, and use the theory with temperature-dependent losses and no heat conduction in the direction of flow. We compute $a = 1.6$ from Eq. (19), leading to $B = 3.527$ from Eq. (23). In Fig. 5 we observe that the solution is on the "fast" flow branch (small a). A perturbation that is large enough might switch to the "choked" solution with same Blow parameter (same heat source, same pressure difference). The temperature difference between inlet and outlet jumps to seven times its previous value ($a = 9.978$). This type of "switch," should it happen, may cause local failure of the absorber.

Consider now the same absorber, but with a higher irradiance; this could correspond, for example, to a location near the center of the absorber, while the previous case is located near the outer rim. If we expect the absorber to operate under the same pressure difference with this higher source, then we obtain only the "choked" solution. In order to maintain the same Blow parameter and the same temperature profile at the higher irradiance, it is necessary to increase the pressure drop. To ensure proper operation of the entire absorber, however, it is then necessary to supply the pressure drop that is required at the point of maximum flux, and throttle all other locations (Buck et al., 1991) so that they "see" a lower pressure drop.

Experimentalists have already discovered the need for adjusting the pressure differences at different absorber locations (Fricker et al., 1988), but have failed to identify the correlation between irradiance and the required pressure drop. In large-scale central receiver applications the distribution of radiation flux at the focal plane may vary greatly throughout the day. This would require continuous adjustment of the pressure drop over much of the receiver area, a complicated and unreliable procedure. A secondary concentrator will, in general, make the flux distribution more uniform, and reduce the need for pressure adjustments, in addition to the main advantage of reducing re-radiation losses.

Table 1 Data for example volumetric absorber variables

Variable	Value	Notes
p_i	10^5 Pa	open receiver
T_i	300 K	
T_∞	3300 K	radiative black-body losses
ω	0.7	air at high temperature
G	4000 kW/m^2	5000 suns
j	8.3 kg/s · m^2	

5 Conclusions

Our simple model for the steady flow in a volumetric absorber indicates that it has limited capability to sustain irradiation, and the upper limit on allowable heat flux depends on the difference in the squares of the pressures divided by the depth and on the viscosity-temperature relation. This limitation is conveniently expressed in terms of the *Blow parameter*. This behavior originates in the positive feedback coming from the interplay of three different physical phenomena: Viscosity determines the volume flow, with increasing temperature the density decreases and so does the heat capacity. In addition to this limitation, the model taking into account the temperature dependence of the viscosity exhibits multiple steady-state solutions, with the possibility of local failure due to switching.

For safely extracting heat from a volumetric absorber operated at high concentrations of a few thousand suns, the following measures may be required:

(1) using a pressurized loop to achieve a sufficiently high Blow parameter and
(2) controlling the mass flux density or outlet temperature instead of the pressure difference.

In a real receiver, control usually utilizes a single measurement representing the average of the absorber outlet conditions. Individual sections of the absorber, however, flow in parallel subject to a common pressure boundary condition. Thus some sections may tend to the fast and other sections to the choked solution. Additional measures are required therefore to ensure uniformity of the flow and temperature over the entire absorber.

Acknowledgments

The authors would like to thank Dr. Jacob Karni for many helpful discussions. This work was made possible, in part, by a generous gift from the late Prof. A. Sabin.

References

Batchelor, G. K., 1967, *An Introduction to Fluid Dynamics*, Cambridge University Press, Cambridge, UK.

Bohmer, M., and Chaza, C., 1991, "The Ceramic Foil Receiver," *Solar Energy Materials & Solar Cells*, Vol. 24, pp. 182–191.

Buck, R., Muir, J. F., Hogan, R. E., and Skocypec, R. D., 1991, "Carbon Dioxide Reforming of Methane in a Solar Volumetric Receiver," *Solar Energy Materials & Solar Cells*, Vol. 24, pp. 449–463.

Buck, R., 1988, "Tests and Calculations for a Volumetric Ceramic Receiver," *Proc. 4th Int. Symp. Solar Thermal Technology*, Santa Fe, NM.

Fricker, H. W., Winkler, C., Silva, M., and Chavez, J., 1988, "Design and Tests Results of the Wire Receiver Experiment Almeria," *Proc. 4th Int. Symp. Solar Thermal Technology*, Santa Fe, NM.

Heinrich, P., Keintzel, G., and Streuber, C., 1992, "2.5 MWt System Test on Volumetric Air Receiver Technology," *Proc. 6th Int. Symp. Solar Thermal Concentrating Technologies*, Almeria, Spain.

Heller, P., Biehler, T., and Buck, R., 1992, "Simulation and Test Results of a 100 kW Volumetric Air Receiver," *Proc. 6th Int. Symp. Solar Thermal Concentrating Technologies*, Almeria, Spain.

Karni, J., Kribus, A., Rubin, R., Doron, P., and Sagie, D., 1992, "Development of the Porcupine Absorber and a Novel Directly-Irradiated Pressurized Receiver (DIAPR)," *Proc. 1st Meeting SolarPACES Task 3: Solar Technology and Applications*, Almeria, Spain.

Landau, L. D., and Lifschitz, E. M., 1983, *Physikalische Kinetik*, Akademie-Verlag, Berlin.

Menigault, T., Flamant, G., and Rivoire, B., 1991, "Advanced High-Temperature Two-Slab Selective Volumetric Receiver," *Solar Energy Materials & Solar Cells*, Vol. 24, pp. 192–203.

Pitz-Paal, R., Feibig, M., and Cordes, S., 1992, "First Experimental Results From the Test of a Selective Volumetric Air Receiver," *Proc. 6th Int. Symp. Solar Thermal Concentrating Technologies*, Almeria, Spain.

Posnansky, M., and Pylkkanen, T., 1991, "Development and Testing of a Volumetric Gas Receiver for High-Temperature Application," *Solar Energy Materials & Solar Cells*, Vol. 24, pp. 204–209.

Schlichting, H., 1979, *Boundary-Layer Theory*, McGraw-Hill, New York.